

The association of like-charged ions in tunable protic pyrazolium salts

Melek Canbulat Özdemir^{a,*}, Ebru Aktan^b, Onur Şahin^c

^a Department of Environmental Engineering, Middle East Technical University, Ankara 06800, Turkey

^b Department of Chemistry, Faculty of Science, Gazi University, Ankara 06500, Turkey

^c Department of Occupat Health & Safety, Faculty of Health Sciences, Sinop University, Sinop 57000, Turkey

ARTICLE INFO

Article history:

Received 10 February 2021

Revised 7 May 2021

Accepted 8 May 2021

Available online 18 May 2021

Keywords:

Tunable protic salts

Pyrazolium

Like-charge attraction

Crystal structure

DFT-D3 calculations

ABSTRACT

The association of like-charged ions is an elusive concept due to the lack of supporting experimental evidence. In the present work, 3,5-dimethyl-1-(p-substitutedphenyl)pyrazolium hexafluorophosphate (p-Cl (2a), p-Br (2b), p-OCH₃ (2c)) tunable protic pyrazolium salts have been synthesized and characterized. The association of like-charged ions in the synthesized salts was observed, as evidenced by X-ray structure analysis of single crystals. The effect of the p-substituent on the association of like-charged ions has been investigated. DFT-D3 studies were performed to unravel the links between the experimentally obtained X-ray results for the solid phase and theoretically calculated results for an isolated system in the gas phase. Additionally, infrared analysis and molecular electrostatic potential analysis were conducted using DFT-D3 to get further information.

© 2021 Elsevier B.V. All rights reserved.

1. Introduction

The electrostatic attraction of oppositely charged ions that gives rise to the formation of ion pairs is a well-known theory in chemistry. Contrarily, the formation of ion pairs between like-charged ions appears as a rare and contradictory concept for which limited experimental evidence exists [1,2]. The pairing of like-charged ions was detected for aqueous mixed electrolyte solutions of tetramethylammonium ions [3], for guanidinium ions in water [4], for metastable colloidal crystallites [5], and certain ionic liquids (ILs) [6–9]. In principle, the cation–cation interactions of organic species might be probable by sufficient delocalization of charge in the cation and the existence of weakly coordinating anions [6,10]. The self-association of simple organic cations through hydrogen bonding was first reported for 4-oxopiperidinium salts with weakly coordinating anions, as evidenced by their X-ray structure analysis [10].

Ionic liquids are organic salts consisting entirely of ions and find particular applications in various fields due to their unique properties [11–15]. Protic ionic liquids (PILs) or protic molten salts (with melting points up to 200 °C), the subclass of ILs, are readily obtained by transferring a proton from particular Brønsted acid to a suitable Brønsted base. Despite their facile synthesis, PILs show complex structural behaviors due to the exchangeable proton on

their cation [16–22]. The strength of interactions present between the ions of ILs, such as Coulomb forces, hydrogen bonding, and dispersion forces, typically determines their structures and properties [23]. The effect of hydrogen bonding on the properties of ionic liquids/salts, has been studied in detail [24–28]. Besides, recent ab initio molecular dynamic calculations of 1,2,4-triazolium and 1,3-dimethylimidazolium cations have confirmed the existence of π -type interactions between ionic species [29–31]. The π - π ring stacking interactions between the cations of ionic liquids/salts have also been observed experimentally by examining their single-crystals through X-ray diffraction analysis. Accordingly, these interactions have been detected for imidazo-pyridine based ionic liquid ([ImPr][TFA], melting point 83–85 °C), for imidazolium picrate salt (mmimPic, melting point 147.5 °C), and for anilinium-based salts (2a, 3a, and 3c with melting points 116.9 °C, 131.5 °C, and 125.2 °C, respectively) [32–34]. Further, head-to-tail dimers of cations have been observed for the tailored palladate tunable aryl alkyl ionic liquid (3d, melting point 108 °C) due to π -stacking of the neighboring phenyl rings [35].

The aim of the present study is to assess the interactions between ions of pyrazolium based tunable protic salts. In our previous work, pyrazolium based tunable protic ionic liquids/salts were synthesized, and solid-state structures of two salts (2a and 3d) were determined by X-ray diffraction analysis [36]. Thus, in continuation of our studies, new 3,5-dimethyl-1-(p-substitutedphenyl)pyrazolium based tunable protic salts (2a–2c), which all include weakly coordinating hexafluorophosphate anion,

* Corresponding author.

E-mail address: ozmelek@metu.edu.tr (M. Canbulat Özdemir).

have been synthesized. The structures of the salts were confirmed by appropriate spectroscopic methods (^1H , ^{13}C , and ^{19}F NMR, FTIR) and elemental analysis. The experimental evidence of the association of like-charged ions in synthesized salts was demonstrated through single-crystal X-ray diffraction analysis (SCXRD). Dispersion-corrected density functional theory (DFT-D3) studies were also conducted to compare experimentally obtained and theoretically calculated results [37].

2. Experimental section

2.1. Materials and instrumentation

All the reagents and solvents were supplied commercially and handled as received. Acetic acid (glacial), acetylacetone, acetonitrile, 4-chlorophenylhydrazine hydrochloride (for synthesis), 4-bromophenylhydrazine hydrochloride (for synthesis), 4-methoxyphenylhydrazine hydrochloride (for synthesis), ethyl acetate, ethanol (absolute), sodium chloride, n-hexane were obtained from Merck. Sodium bicarbonate, sodium sulfate, and hexafluorophosphoric acid (~55 wt.% in H_2O) were purchased from Sigma Aldrich.

The synthesis of 3,5-dimethyl-1-(p-substitutedphenyl)-1H-pyrazole derivatives (1a-1c) was carried out under microwave irradiation by the multimode oven (Microsynth-Milestone). NMR spectra (^1H , ^{13}C , ^{19}F) of the salts (2a-2c) were recorded on a Bruker Avance 300 Ultra-Shield spectrometer. FTIR spectra of all compounds were acquired with a "Thermo Fischer Scientific Nicolet iS10 FTIR" spectrometer. Their melting points were measured by the "Electrothermal 9200" melting point apparatus and were not corrected. The elemental analysis of the salts was obtained by the "LECO, CHNS-932" elemental analyzer.

2.2. Synthesis and characterization of the pyrazolium based tunable protic salts (2a-2c)

The appropriate 3,5-dimethyl-1-(p-substitutedphenyl)-1H-pyrazole compound (1a-1c) (5 mmol), which was synthesized under MW irradiation by following a reported procedure [36], was dissolved in ethanol (5 mL). Hexafluorophosphoric acid (5 mmol, 55% in water) was added dropwise to the solution stirring at room temperature, and continued to stir for 30 min. The solid formed was collected by filtration, dissolved in acetonitrile (10 mL), and refluxed with active charcoal. After filtration, the solvent was evaporated. Their single crystals were acquired by slow evaporation of ethanol solutions of the salts.

1-(p-chlorophenyl)-3,5-dimethylpyrazolium hexafluorophosphate (2a): FTIR (ATR, cm^{-1}) ν_{max} = 3424, 3115, 2987, 2927, 1601, 1550, 1495, 1413, 1093, 846, 555. $^1\text{H-NMR}$ (CDCl_3 , ppm): δ = 2.33 (s, 3H, $-\text{CH}_3$), 2.43 (s, 3H, $-\text{CH}_3$), 6.27 (s, 1H, $-\text{CH}$), 7.40–7.43 (d, 2H, pH, J = 8.8 Hz), 7.51–7.54 (d, 2H, pH, J = 8.8 Hz). $^{13}\text{C-NMR}$ (CDCl_3 , ppm) δ = 11.66, 11.88, 108.30, 127.05, 130.14, 133.06, 136.46, 144.31, 147.85. $^{19}\text{F-NMR}$ (CDCl_3 , ppm): $-\text{70.58}$, $-\text{73.11}$. Analysis: calcd for $\text{C}_{22}\text{H}_{23}\text{Cl}_2\text{F}_6\text{N}_4\text{P}$: C 47.24 H 4.14 N 10.02. Found: C 46.74 H 4.11 N 9.93. Yield: 80 % (white crystal), M.p: 117 °C.

1-(p-bromophenyl)-3,5-dimethylpyrazolium hexafluorophosphate (2b): FTIR (ATR, cm^{-1}) ν_{max} = 3423, 3144, 3107, 2971, 2925, 1597, 1549, 1491, 1408, 1071, 843, 555. $^1\text{H-NMR}$ (DMSO-d_6 , ppm): δ = 2.17 (s, 3H, $-\text{CH}_3$), 2.30 (s, 3H, $-\text{CH}_3$), 6.09 (s, 1H, $-\text{CH}$), 7.45–7.48 (d, 2H, pH, J = 8.7 Hz), 7.66–7.69 (d, 2H, pH, J = 8.7 Hz). $^{13}\text{C-NMR}$ (DMSO-d_6 , ppm) δ = 12.56, 13.56, 108.11, 120.27, 126.41, 132.47, 138.96, 140.25, 148.64. $^{19}\text{F-NMR}$ (CDCl_3 , ppm): $-\text{70.41}$, $-\text{72.97}$. Analysis: calcd for $\text{C}_{22}\text{H}_{23}\text{Br}_2\text{F}_6\text{N}_4\text{P}$: C 40.76 H 3.58 N 8.64. Found: C 40.25 H 3.68 N 8.54. Yield: 82 % (white crystal), M.p: 141 °C.

Table 1
Crystal data and structure refinement parameters for 2a–2c.

	2a	2b	2c
Empirical formula	$\text{C}_{22}\text{H}_{23}\text{N}_4\text{Cl}_2\text{PF}_6$	$\text{C}_{22}\text{H}_{23}\text{N}_4\text{Br}_2\text{PF}_6$	$\text{C}_{24}\text{H}_{29}\text{N}_4\text{O}_2\text{PF}_6$
Formula weight	559.31	648.23	550.48
Crystal system	Monoclinic	Monoclinic	Monoclinic
Space group	$\text{P}2_1/\text{n}$	$\text{C}2/\text{c}$	$\text{C}2/\text{c}$
a (Å)	8.9958 (6)	8.9324 (7)	9.4422 (11)
b (Å)	23.5782 (17)	21.0010 (18)	21.107 (3)
c (Å)	11.7593 (9)	13.4307 (11)	13.3039 (13)
β (°)	91.057 (2)	94.227 (3)	96.654 (5)
V (Å ³)	2493.8 (3)	2512.6 (4)	2633.6 (5)
Z	4	4	4
D_c (g cm^{-3})	1.490	1.714	1.388
μ (mm^{-1})	0.39	3.35	0.18
θ range (°)	3.1–26.2	3.0–28.3	3.6–26.2
Measured reffs.	41,730	20,454	27,769
Independent reffs.	4579	2327	2730
R_{int}	0.073	0.066	0.054
S	1.06	1.13	1.15
R1/wR2	0.104/0.219	0.070/0.128	0.065/0.153
$\Delta\rho_{\text{max}}/\Delta\rho_{\text{min}}$ ($\text{e}\text{Å}^{-3}$)	0.57/−0.47	0.52/−0.41	0.21/−0.28

3,5-dimethyl-1-(p-methoxyphenyl)pyrazolium hexafluorophosphate (2c): FTIR (ATR, cm^{-1}) ν_{max} = 3444, 3144, 2970, 1598, 1513, 1453, 1318, 1257, 1171, 1039, 848, 555. $^1\text{H-NMR}$ (CDCl_3 , ppm): δ = 2.28 (s, 3H, $-\text{CH}_3$), 2.35 (s, 3H, $-\text{CH}_3$), 3.88 (s, 3H, $-\text{OCH}_3$ -pH), 6.19 (s, 1H, $-\text{CH}$), 7.0–7.03 (d, 2H, pH, J = 8.9 Hz), 7.29–7.32 (d, 2H, pH, J = 8.9 Hz). $^{13}\text{C-NMR}$ (CDCl_3 , ppm): δ = 11.83, 12.06, 55.70, 107.44, 114.89, 127.15, 128.51, 143.54, 147.65, 160.53. $^{19}\text{F-NMR}$ (CDCl_3 , ppm): $-\text{70.79}$, $-\text{73.32}$. Analysis: calcd for $\text{C}_{24}\text{H}_{29}\text{F}_6\text{N}_4\text{O}_2\text{P}$: C 52.36 H 5.31 N 10.18. Found: C 52.30 H 5.28 N 10.20. Yield: 90 % (white crystal), M.p: 133 °C.

2.3. X-ray diffraction analysis

The data collection was performed on a D8-QUEST diffractometer equipped with graphite-monochromatic Mo- $K\alpha$ radiation by selecting suitable crystals of 2a-2c at 296 K. The structures of the salts were solved by direct methods using SHELXS-2013 [38] and refined by full-matrix least-squares methods on F^2 using SHELXL-2013 [39]. All non-hydrogen atoms were refined with anisotropic parameters. The H atom of the N atom was located in a difference map and refined freely. The other H atoms were located from different maps and then treated as riding atoms with a C-H distance of 0.93–0.96 Å. The following procedures were implemented in our analysis: data collection: Bruker APEX2 [40]; the program used for molecular graphics were as follows: MERCURY programs [41]; software used to prepare material for publication: WinGX [42]. Details of data collection and crystal structure determinations are given in Table 1.

2.4. Quantum chemical calculations

The molecular geometry optimizations and the maps of molecular electrostatic potential (MEP) of the 3,5-dimethyl-1-(p-substitutedphenyl)pyrazolium hexafluorophosphates (2a-2c) were carried out using a 6-31G(d) basis set in which B3LYP-D3 functional were implemented in the gas phase. Each optimized structure of the salts was confirmed to be local minima on the potential energy surface through vibrational frequency analysis to prevent imaginary frequencies. The geometry optimizations of the salts were conducted based on their crystal structures using the Gaussian 09 program package [43].

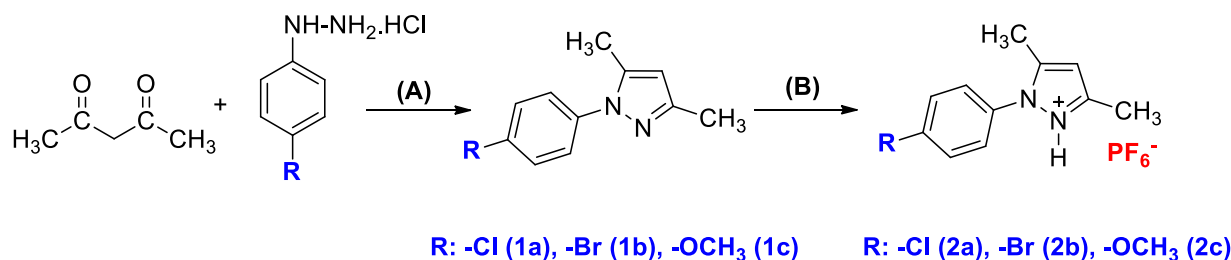


Fig. 1. The synthetic path for the preparation of the pyrazolium based tunable protic salts (A) Acetic acid, MW, 120 °C; (B) Ethanol, HPF₆ (55% in water), R.T.

3. Results and discussion

3.1. Synthesis and characterization

The syntheses of pyrazolium based tunable protic salts (2a–2c) were performed via a two-step reaction, as outlined in Fig. 1. In the first step, proper arylhydrazine hydrochloride and acetylacetone were used as starting materials to synthesize 1a–1c compounds under MW irradiation. In the second step, the salts were obtained by a Brønsted acid-base reaction between the 1a–1c and hexafluorophosphoric acid in a stoichiometric ratio at room temperature.

The NMR (¹H, ¹³C, ¹⁹F), FTIR, elemental analysis, and single-crystal X-ray diffraction analysis were performed to elucidate the chemical structures of the salts. The NMR and FTIR spectra of the salts are given in Supplementary Materials. The FTIR spectra of the compounds show typical bands belonging to cations of 2a–2c ($\nu(\text{C}=\text{N})$ and $\nu(\text{C}=\text{C})$ stretching vibrations: 1601–1408 cm⁻¹) and hexafluorophosphate anion ($\nu(\text{PF})$: 848–843 cm⁻¹). ¹H-NMR spectra of the salts show the signals compatible with the aliphatic and aromatic protons of the pyrazolium cations. Besides, the peaks of carbon atoms, observed in ¹³C-NMR spectra, are compatible with the expected structures of the synthesized compounds. Their ¹⁹F-NMR spectra show typical doublets at ca. δ (–70,15 ppm) (–73.32 ppm) due to the octahedral geometry of hexafluorophosphate anion.

3.2. Crystal structures of the pyrazolium based tunable protic salts

The association of like-charged ions in the pyrazolium based tunable protic salts has been observed by single-crystal X-ray diffraction analysis. The SCXRD experiment has established that the 2a crystallizes in the monoclinic crystal system with space group P2₁/n (Table 1). The asymmetric unit of 2a consists of one cation, one neutral pair, and one hexafluorophosphate anion, as shown in Fig. 2a. The cation-neutral pairs produce N-H...N hydrogen bond (Table 2), and they are also part of a hydrogen bond network connecting all building units to an extensive one-dimensional hydrogen-bonded lattice. The combination of the N-H...N hydrogen bond between the cation and neutral pair and C-H...F hydrogen bond between the cation and [PF₆⁻] anion produces a chain along [010] direction (Fig. 2b). As illustrated in Fig. 2c, the molecules of 2a are connected by C-H... π and π ... π interactions (Table 3). The asymmetric unit also includes [PF₆⁻] anion, which charge-counterbalances the cation molecule.

The 2b and 2c compounds crystallize in the monoclinic crystal system with space group C2/c (Table 1). In the crystals of 2b and 2c, the asymmetric units consist of one cation molecule and half hexafluorophosphate anion (Fig. 3a and 3b). Additionally, in 2a, all atoms are located in general positions, while the phosphorus atom of hexafluorophosphate anion is located on a 2-fold inversion center in 2b and 2c.

As shown in Fig. 4a, the cations of 2b compound are connected by C-H... π and π ... π interactions. The H11A atom of C11

Table 2

Hydrogen bonds parameters for 2a–2c (Å, °).

D-H...A	D-H	H...A	D...A	D-H...A
2a				
C6-H6...F2	0.93	2.50	3.165 (7)	129
C19-H19...F6 ⁱ	0.93	2.43	3.322 (8)	161
N2-H2A...N4	0.91 (7)	1.86 (7)	2.755 (7)	168
C22-H22C...Cg(1)	0.96	2.93	3.583 (7)	126
2b				
C8-H8...F3 ⁱⁱ	0.93	2.53	3.277 (7)	137
C11-H11A...Cg(1) ⁱ	0.96	2.99	3.866 (7)	152
2c				
C9-H9...F3 ⁱⁱ	0.93	2.44	3.230 (3)	143
C11-H11C...O1 ⁱⁱⁱ	0.96	2.49	3.360 (4)	150

Symmetry code: (i) $-x + 1/2, y + 1/2, -z + 1/2$; Cg(1)=C1-C6 for 2a; (ii) $1-x, 1-y, 1-z$; (iii) $x + 1, y, z$; Cg(1)=C7/C9-N2-N1 for 2b; (ii) $x - 1, y, z$; (iii) $-x + 3/2, -y + 1/2, -z + 1$ for 2c.

Table 3

π ... π interactions distances for 2a–2c (Å).

Cg(I)	Cg(J)	Cg-Cg	Perpendicular distance
2a			
Cg(1)	Cg(1) ⁱ	3.772 (3)	3.355
2b			
Cg(2)	Cg(2) ⁱ	3.993 (3)	3.570
2c			
Cg(1)	Cg(1) ⁱ	4.023 (2)	3.679

Symmetry codes: (i) $1-x, 1-y, 1-z$; Cg(1)=C1-C6 for 2a; (ii) $1/2-x, 1/2-y, 1-z$; Cg(2)=C1-C6 for 2b; (i) $3/2-x, 1/2-y, 1-z$; Cg(1)=C1-C6 for 2c.

in the molecule at (x, y, z) acts as a hydrogen-bond donor to the C7/C9-N2-N1 ring in the molecule at (x + 1, y, z), so forming a centrosymmetric R₂²(8) ring motifs (Table 2). Besides, an intermolecular π ... π interaction occurs between the two symmetry-related phenyl rings of neighboring molecules (Table 3). Thus, the combination of C-H... π and π ... π interactions produce a chain along [110] direction. In the crystal of 2c, unlike from 2b, C-H...O hydrogen-bonds produce a centrosymmetric R₂²(18) ring motifs because of the methoxy substituent at the para position of the phenyl ring. The combination of π ... π interactions, C-H...O hydrogen bonds between the cations and C-H...F hydrogen bonds between the cations and anions produce a chain along [101] direction (Fig. 4b, Tables 2 and 3).

3.3. Geometric optimizations of pyrazolium based tunable protic salts

In the optimized geometry of 2a, calculated at the B3LYP-D3/6-31G(d) level in the gas phase, classical hydrogen bonding interactions between fluorine atoms of [PF₆⁻] anion and the hydrogen atoms of pyrazolium cation were observed (Fig. 5a). Based on the obtained results, the hydrogen bond lengths of F52...H8, F53...H26, and F54...H8 were found as 2.36 Å, 2.39 Å, and 2.32 Å, respectively. Additionally, the N-H...N hydrogen bond produced by the cation-neutral pairs, detected in the SCXRD experiment, was also

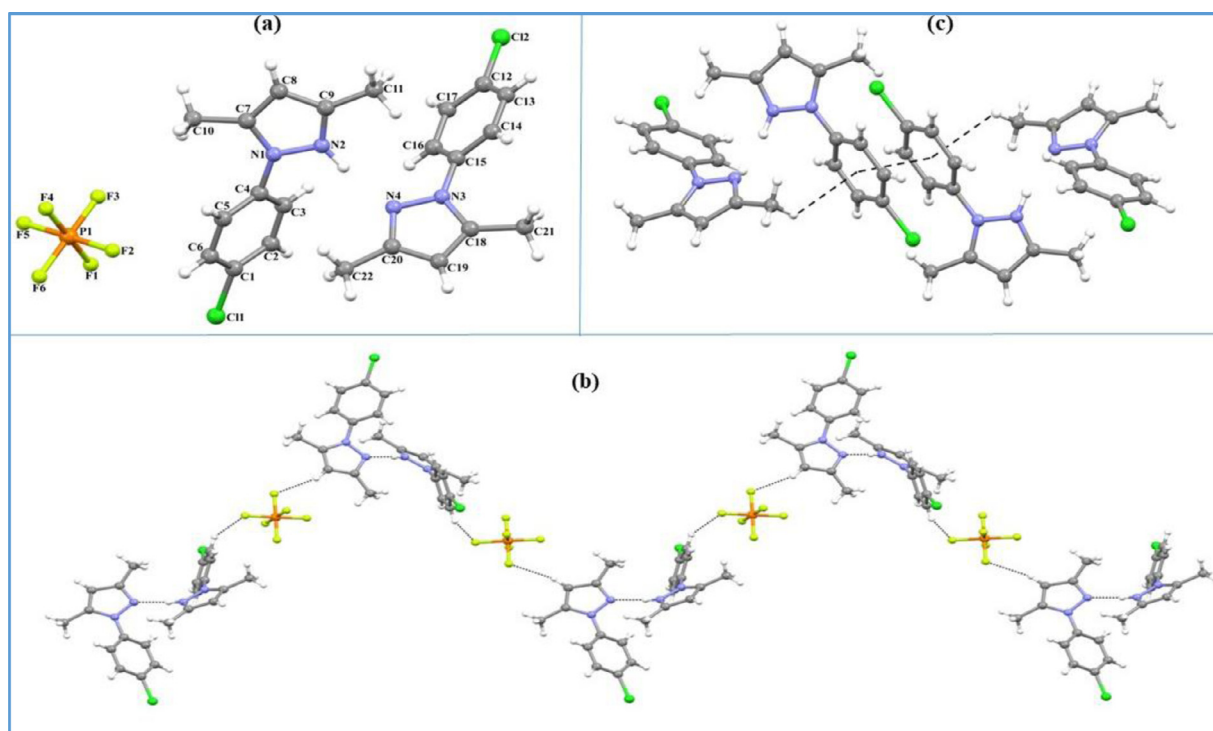


Fig. 2. (a) The molecular structure of **2a** showing the atom numbering scheme (b) Crystal structure of **2a**, showing the formation of a chain along [010] generated by N-H...N and C-H...F hydrogen bonds (c) Crystal structure of **2a**, showing the formation of C-H... π and π ... π interactions.

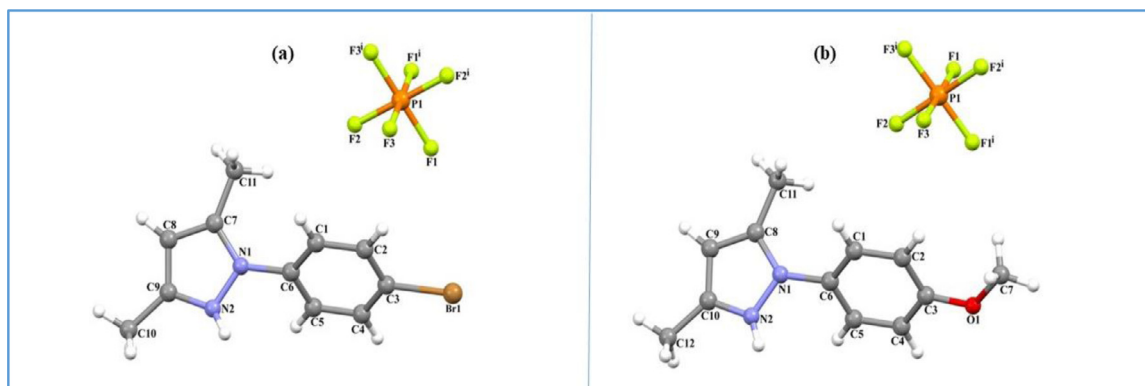


Fig. 3. (a) The molecular structure of **2b** showing the atom numbering scheme. [(i) $-x, y, -z + 3/2$] (b) The molecular structure of **2c** showing the atom numbering scheme. [(i) $-x + 2, y, -z + 1/2$].

observed theoretically. The hydrogen bond distance of H26...N51 was calculated as 1.76 Å (exp. 1.86 Å), and the angle value of N25-H26...N51 was calculated as 175° (exp. 168°).

As seen in Fig. 5b, the optimized geometry of **2b** is consistent with its crystal structure depicted in Fig. 6. The bond lengths of C19-H20 and C44-H45 were found to be 0.93 Å in the SCXRD experiment and 1.08 Å in theoretical calculations. The H20...F1, H28...F1, and H45...F3 hydrogen bond lengths were calculated 2.32 Å (exp. 2.53 Å), 2.27 Å and 2.30 Å, respectively. The theoretical angle value of C19-H20...F1 was found as 134° (exp. 137°). According to theoretical calculations, C8-C17-N30-C21 and C33-C42-N55-C46 dihedral angles were 41°.

The optimized geometry of **2c** calculated at the B3LYP-D3/6-31G(d) level in the gas phase is given in Fig. 5c. The hydrogen bond length of H67...F31 was calculated as 1.71 Å. The calculated bond length of hydrogen-bonded N-H (N64-H67) was found as 1.034 Å, and this value was higher than free N-H (N28-H66) (1.026 Å), as expected. The distances of H20...O63 and H65...O27 were calcu-

lated as 2.60 Å and 2.32 Å, respectively. The corresponding experimental value of H20...O63 length was observed as 2.49 Å. The theoretical angle value of C41-H42...O27 was found as 155° (exp. 150°). The X-ray crystal structure and DFT calculations at the B3LYP/6-31+G(d) level of theory, including D3 dispersion correction, show that hydrogen bonding between the cations of the **2c** overcomes the repulsive Coulomb forces [6,8].

3.3.1. Vibrational spectra

The vibrational frequencies of the salts (**2a**, **2b** and **2c**) were obtained theoretically and experimentally in the spectral region of 4000 to 500 cm^{-1} . The calculated frequencies must be multiplied by the scaling factors since the calculated harmonic frequencies are higher than those observed experimentally. The differences between calculated and experimental frequencies arise from basis set defects, neglecting anharmonic effects, and electron correlation [44-46]. Thus, the B3LYP-D3/6-31G(d) calculated vibrational frequencies are calibrated with the scaling factor 0.9642. The experi-

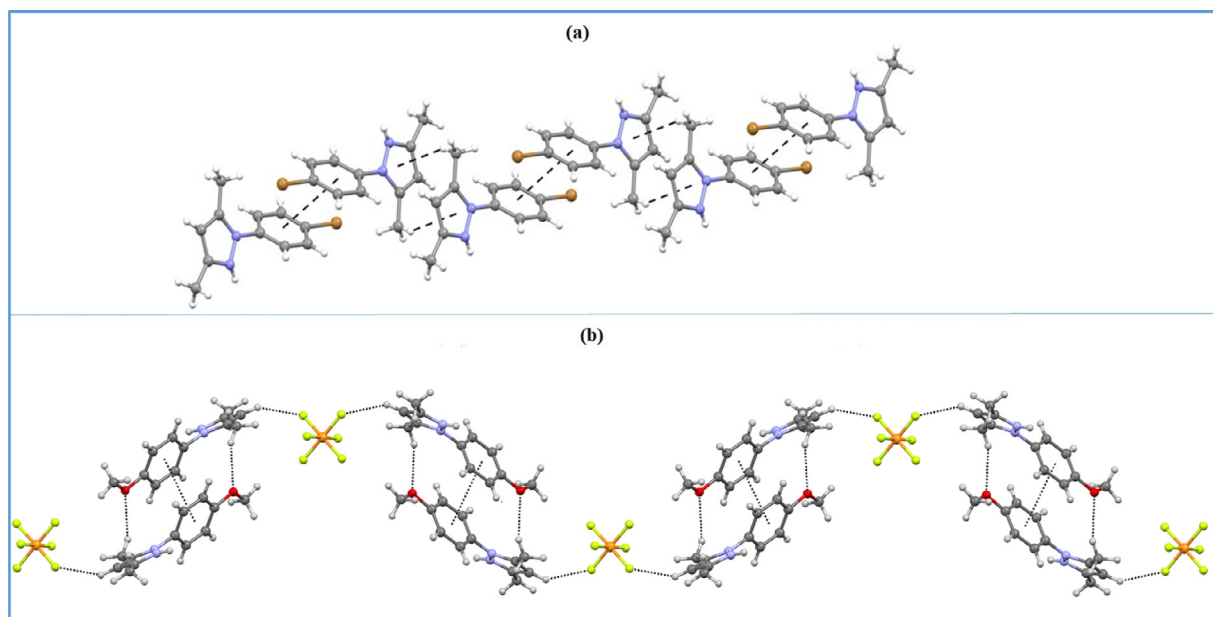


Fig. 4. (a) Crystal structure of **2b**, showing the formation of a chain along [110] generated by C-H... π and π ... π interactions (b) Crystal structure of **2c**, showing the formation of a chain along [101] generated by π ... π interactions, C-H...O and C-H...F hydrogen bonds.

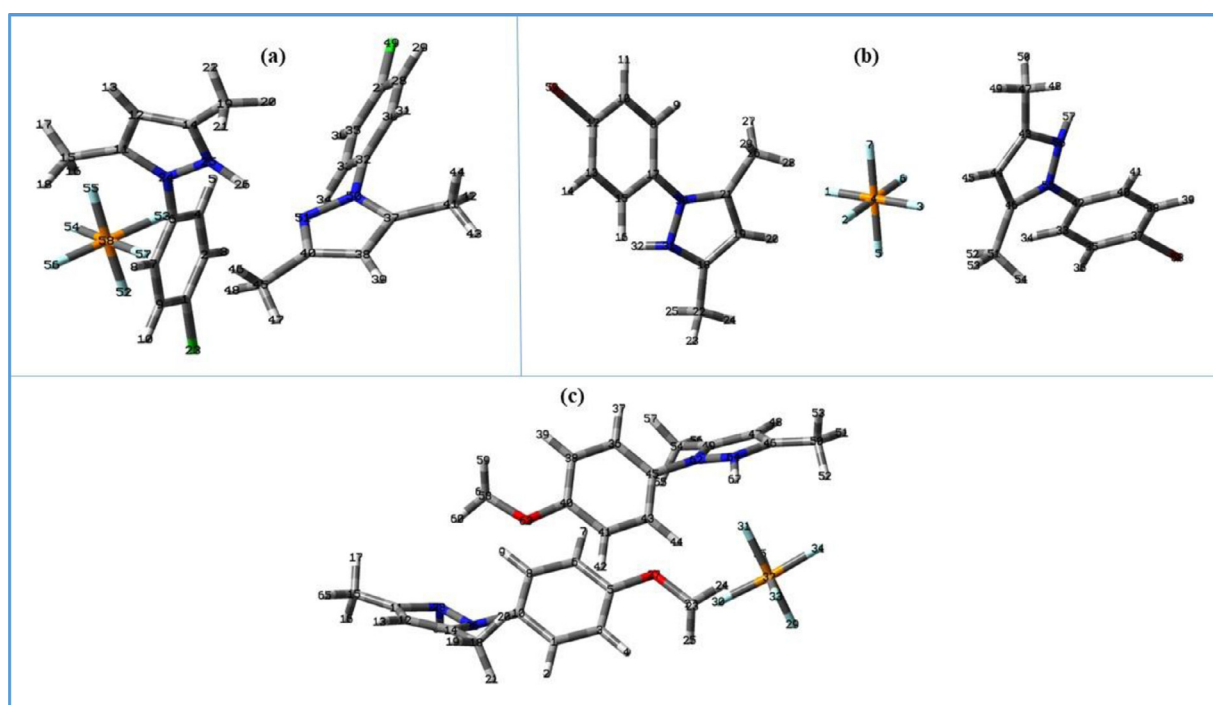


Fig. 5. (a) The optimized geometry of **2a**, (b) the optimized geometry of **2b**, (c) the optimized geometry of **2c**, calculated at B3LYP-D3/6-31G(d) level in the gas phase.

mentally scaled vibrational frequencies and assignments of fundamental vibrational bands of the synthesized compounds are given in Supp. Table 1.

The free NH and hydrogen-bonded NH stretching bands of the salts were observed at two different wavenumbers in their FTIR spectra (Supp. Table 1). The free N-H stretching vibrations of the **2a**, **2b** and **2c** were observed as weak intensity bands at 3749 cm^{-1} (calc.no observation), 3750 cm^{-1} (calc. 3353 cm^{-1}), and 3711 cm^{-1} (calc. 3211 cm^{-1}), respectively. On the other hand, the hydrogen-bonded NH stretchings were observed as very weak intensity bands at 2927 cm^{-1} (calc. 2797 cm^{-1}) for **2a** (N25-H26...N51) and

3444 cm^{-1} (calc. 3157 cm^{-1}) for **2c** (N64-H67...F31). The hydrogen-bonded N-H was not observed for **2b**.

The CH_3 asymmetric stretching vibrations were observed experimentally as very weak and weak bands between 2987 cm^{-1} –2970 cm^{-1} and theoretically between 3029 cm^{-1} –2991 cm^{-1} . The C = C, C = N, and N = N stretching vibrations appear in the region 1605 cm^{-1} –1414 cm^{-1} (exp.1601 cm^{-1} –1408 cm^{-1}) and show usually mixing with the CH_3 scissoring. The O- CH_3 symmetric stretchings of compound **2c** assigned at 1257 cm^{-1} as a very strong and at 1249 cm^{-1} as a weak intensity band (corresponding calculated values are 1264 cm^{-1} and 1248 cm^{-1}). The C-Cl stretching was ob-

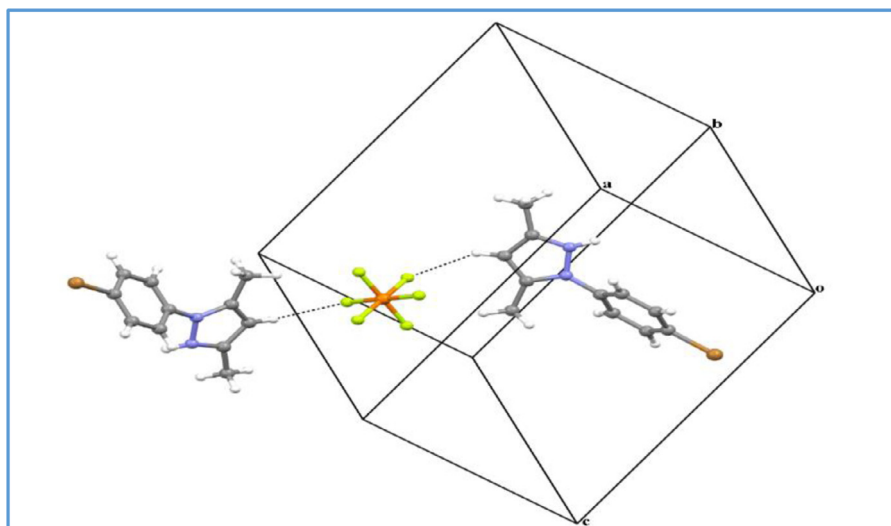


Fig. 6. Crystal structure of **2b**, showing the formation of C-H...F hydrogen bonds.

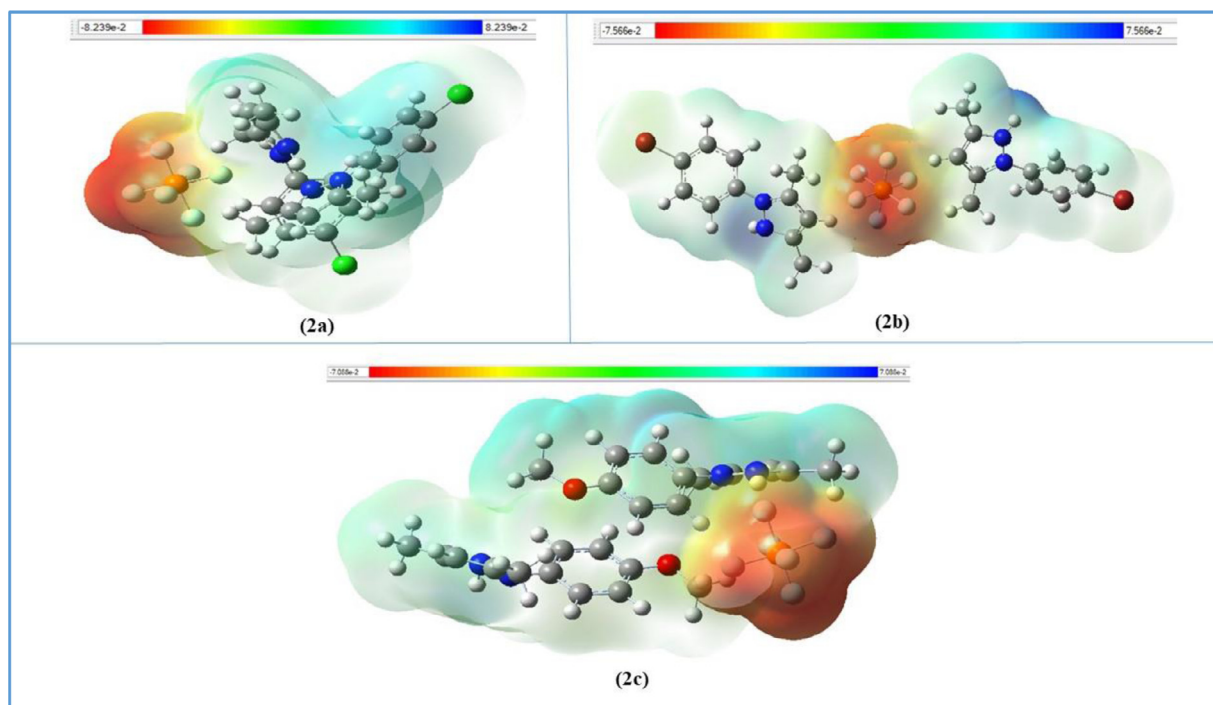


Fig. 7. MEP plots of **2a**, **2b**, and **2c** obtained at the B3LYP-D3/6-31G(d) level of the theory (For interpretation of the references to color in this figure, the reader is referred to the web version of this article.).

served at 506 cm^{-1} (calc. 502 cm^{-1}) for **2a** as a medium band. The band at 647 cm^{-1} (calc. 680 cm^{-1}) can be assigned as a C-Br stretching band for **2b**. The very strong bands observed at 846 cm^{-1} for **2a** (calc. 857 cm^{-1}), 843 cm^{-1} for **2b** (calc. 891 cm^{-1}) and 848 cm^{-1} for **2c** (calc. 863 cm^{-1}) can be assigned as F-P-F symmetric stretchings.

3.3.2. Molecular electrostatic potential (MEP) maps

The maps of the molecular electrostatic potential surface for the ground state geometry of the molecules provide information about their electrophilic and nucleophilic regions [47,48]. The MEP maps of the pyrazolium based tunable protic salts were obtained at the B3LYP-D3/6-31G(d) level of theory. As seen in Fig. 7, the negative potential sites (red color) of the salts are located on $[\text{PF}_6]^-$ anion and distribute on fluorine atoms. The positive potential sites (blue

color) are located on NH hydrogen atoms of the 3,5-dimethyl-1-(*p*-substitutedphenyl)pyrazolium cations.

Conclusion

In this work, we report the association of ions in 3,5-dimethyl-1-(*p*-substitutedphenyl)pyrazolium hexafluorophosphate tunable protic salts by X-ray analysis of single crystals. Based on the obtained results, the hydrogen bonding and π -type interactions between the ions of the synthesized salts have significant effects on the arrangement of their crystal structures. It is also observed that the combination of intermolecular interactions that lead to the association of the cations varies depending on the *p*-substituent at the phenyl ring of the pyrazolium cation. Accordingly, for the **2a**; C-H... π and π ... π interactions and the N-H...N

hydrogen bond between the cation and neutral pair, for the 2b; C-H... π and π ... π interactions between the two symmetry-related phenyl rings of neighboring cations, and for the 2c; π ... π interactions and C-H...O hydrogen bonds between the cations are responsible for the association of the cations of the salts. The theoretical calculations based on the crystal structures of the salts also show that the obtained bond length and dihedral angles are consistent with the experimental results.

It is known that the understanding of intermolecular interactions between the ions of ionic liquids/salts are crucial to obtain the compounds with desired features for specific applications. Thus, we believe that the findings of this study will contribute to the field related to the synthesis of new tunable ionic liquids/salts with desired properties.

Appendix A. supplementary data

Crystallographic data for the structural analysis have been deposited with the Cambridge Crystallographic Data center, CCDC No. 1893265 for **2a**, 1877558 for **2b**, and 1893266 for **2c**. Copies of this information may be obtained free of charge from the Director, CCDC, 12 Union Road, Cambridge CB2 1EZ, UK (fax: +44-1223-336,033; e-mail: deposit@ccdc.cam.ac.uk or www: <http://www.ccdc.cam.ac.uk>).

Funding

This research did not receive any specific grant from funding agencies in the public, commercial, or not-for-profit sectors.

Declaration of Competing Interest

All authors declare that they have no known competing financial interests or personal relationships that could have appeared to influence the work reported in this paper.

CRediT authorship contribution statement

Melek Canbulat Özdemir: Investigation, Writing - original draft, Methodology, Data curation, Formal analysis, Visualization. **Ebru Aktan:** Investigation, Writing - original draft, Data curation, Visualization. **Onur Şahin:** Investigation, Writing - original draft, Data curation, Visualization.

Acknowledgments

The authors acknowledge to Scientific and Technological Research Application and Research Center, Sinop University, Turkey, for the use of the Bruker D8 QUEST diffractometer. The theoretical calculations reported in this paper were performed at TUBITAK ULAKBIM, High Performance and Grid Computing Center (TRUBA resources).

Supplementary materials

Supplementary material associated with this article can be found, in the online version, at doi:10.1016/j.molstruc.2021.130684.

References

- [1] Y. Marcus, G. Hefter, Ion pairing, *Chem. Rev.* 106 (2016) 4585–4621, doi:10.1021/cr040087x.
- [2] T. Niemann, P. Stange, A. Strate, R. Ludwig, Like-likes-like: cooperative hydrogen bonding overcomes coulomb repulsion in cationic clusters with net charges up to $Q=+6e$, *Chem. Phys. Chem.* 19 (2018) 1691–1695, doi:10.1002/cphc.201800293.
- [3] M. Holz, K.J. Patil, Cation-cation association of tetramethylammonium ions in aqueous mixed electrolyte solutions, *Ber. Bunsen Ges.* 95 (1991) 107–113, doi:10.1002/bbpc.19910950201.
- [4] O. Shih, A.H. England, G.C. Dallinger, J.W. Smith, K.C. Duffey, R.C. Cohen, D. Prendergast, R.J. Saykally, Cation-cation contact pairing in water: guanidinium, *J. Chem. Phys.* 139 (2013) 035104, doi:10.1063/1.4813281.
- [5] A.E. Larsen, D.G. Grier, Like-charge attractions in metastable colloidal crystallites, *Nature* 385 (1997) 230–233, doi:10.1038/385230a0.
- [6] A. Knorr, R. Ludwig, Cation-cation clusters in ionic liquids: cooperative hydrogen bonding overcomes like-charge repulsion, *Sci. Rep.* 5 (2015) 175051–175057, doi:10.1038/srep17505.
- [7] A. Knorr, P. Stange, K. Fumino, F. Weinhold, R. Ludwig, Spectroscopic evidence for clusters of like-charged ions in ionic liquids stabilized by cooperative hydrogen bonding, *Chem. Phys. Chem.* 17 (2016) 458–462, doi:10.1002/cphc.201501134.
- [8] A. Strate, T. Niemann, D. Michalik, R. Ludwig, When like-charged ions attract in ionic liquids: controlling the formation of cationic clusters by the interaction strength of the counterions, *Angew. Chem. Int. Ed.* 56 (2017) 496–500, doi:10.1002/anie.201609799.
- [9] M. Campetella, A.L. Donne, M. Daniele, L. Gontrani, S. Lupi, E. Bodo, F. Leonelli, Hydrogen bonding features in cholinium-based protic ionic liquids from molecular dynamics simulations, *J. Phys. Chem. B* 122 (2018) 2635–2645, doi:10.1021/acs.jpcc.7b12455.
- [10] W. Gamrad, A. Dreier, R. Goddard, K.R. Pörschke, Cation-cation pairing by N-C-H...O hydrogen bonds, *Angew. Chem. Int. Ed.* 54 (2015) 4482–4487, doi:10.1002/anie.201408278.
- [11] S.K. Singh, A.W. Savoy, Ionic liquids synthesis and applications: an overview, *J. Mol. Liq.* 297 (2020) 112038, doi:10.1016/j.molliq.2019.112038.
- [12] X. Zhang, W. Xiong, M. Shi, Y. Wu, X. Hu, Task-specific ionic liquids as absorbents and catalysts for efficient capture and conversion of H_2S into value-added mercaptan acids, *Chem. Eng. J.* 408 (2021) 127866, doi:10.1016/j.cej.2020.127866.
- [13] C.A. Angell, Y. Ansari, Z. Zhao, Ionic liquids: past, present and future, *Faraday Discuss.* 154 (2012) 9–27, doi:10.1039/C1FD00112D.
- [14] K.E. Gutowski, Industrial uses and applications of ionic liquids, *Phys. Sci. Rev.* (2018) 20170191, doi:10.1515/psr-2017-0191.
- [15] X. Zhang, W. Xiong, Z. Tu, L. Peng, Y. Wu, X. Hu, Supported ionic liquid membranes with dual-site interaction mechanism for efficient separation of CO_2 , *ACS Sustain. Chem. Eng.* 7 (2019) 10792–10799, doi:10.1021/acssuschemeng.9b01604.
- [16] T.L. Greaves, C.J. Drummond, Protic ionic liquids: properties and applications, *Chem. Rev.* 108 (2008) 206–237 <https://pubs.acs.org/doi/>, doi:10.1021/cr068040u.
- [17] T.L. Greaves, C.J. Drummond, Protic ionic liquids: evolving structure-property relationships and expanding applications, *Chem. Rev.* 115 (2015) 11379–11448, doi:10.1021/acs.chemrev.5b00158.
- [18] T.L. Greaves, K. Ha, B.W. Muir, S.C. Howard, A. Weerawardena, N. Kirby, C.J. Drummond, Protic ionic liquids (PILs) nanostructure and physicochemical properties: development of high-throughput methodology for PIL creation and property screens, *Phys. Chem. Chem. Phys.* 17 (2015) 2357–2365, doi:10.1039/C4CP04241G.
- [19] D. Shang, X. Zhang, S. Zeng, K. Jiang, H. Gao, H. Dong, Q. Yang, S. Zhang, Protic ionic liquid [Bim][NTf₂] with strong hydrogen bond donating ability for highly efficient ammonia absorption, *Green Chem.* 19 (2017) 937–945, doi:10.1039/c6gc03026b.
- [20] K. Fumino, V. Fossog, P. Stange, D. Paschek, R. Hempelmann, R. Ludwig, Controlling the subtle energy balance in protic ionic liquids: dispersion forces compete with hydrogen bonds, *Angew. Chem. Int. Ed.* 54 (2015) 2792–2795, doi:10.1002/anie.201411509.
- [21] M. Campetella, M. Montagna, L. Gontrani, E. Scarpellini, E. Bodo, Unexpected proton mobility in the bulk phase of cholinium-based ionic liquids: new insights from theoretical calculations, *Phys. Chem. Chem. Phys.* 19 (2017) 11869–11880, doi:10.1039/C7CP01050H.
- [22] X. Zhang, W. Xiong, L. Peng, Y. Wu, X. Hu, Highly selective absorption separation of H_2S and CO_2 from CH_4 by novel azole-based protic ionic liquids, *AIChE J.* 66 (2020) e16936, doi:10.1002/aic.16936.
- [23] K. Fumino, T. Peppel, M. Geppert-Rybczynska, D.H. Zaitsau, J.K. Lehmann, S.P. Verevkin, M. Köckerling, R. Ludwig, The influence of hydrogen bonding on the physical properties of ionic liquids, *Phys. Chem. Chem. Phys.* 13 (2011) 14064–14075, doi:10.1039/c1cp20732f.
- [24] C.J. Dymek Jr, D.A. Grossie, A.V. Fratini, W.W. Adams, Evidence for the presence of hydrogen-bonded ion-ion interactions in the molten salt precursor, 1-methyl-3-ethylimidazolium chloride, *J. Mol. Struct.* 213 (1989) 25–34, doi:10.1016/0022-2860(89)85103-8.
- [25] A. Elaiwi, P.B. Hitchcock, K.R. Seddon, N. Srinivasan, Y. Tan, T. Welton, J.A. Zora, Hydrogen bonding in imidazolium salts and its implications for ambient-temperature halogenoaluminate(III) ionic liquids, *J. Chem. Soc. Dalton Trans.* (1995) 3467–3472, doi:10.1039/DT9950003467.
- [26] X.P. Xuan, L.L. Chang, H. Zhang, N. Wang, Y. Zhao, Hydrogen bonds in the crystal structure of hydrophobic and hydrophilic COOH-functionalized imidazolium ionic liquids, *Cryst. Eng. Comm.* 16 (2014) 3040–3046, doi:10.1039/c3ce42492h.
- [27] J. Dupont, On the solid, liquid and solution structural organization of imidazolium ionic liquids, *J. Braz. Chem. Soc.* 15 (2004) 341–350, doi:10.1590/S0103-50532004000300002.
- [28] D. Zhao, Z. Fei, R. Scopelliti, P.J. Dyson, Synthesis and characterization of ionic liquids incorporating the nitrile functionality, *Inorg. Chem.* 43 (2004) 2197–2205, doi:10.1021/ic034801p.

- [29] H. Li, J.A. Boatz, M.S. Gordon, Cation-cation π - π stacking in small ionic clusters of 1,2,4-triazolium, *J. Am. Chem. Soc.* 130 (2008) 392–393, doi:[10.1021/ja076406u](https://doi.org/10.1021/ja076406u).
- [30] Y. Wang, A. Laaksonen, M.D. Fayer, Hydrogen bonding versus π - π stacking interactions in imidazolium-oxalato-borate ionic liquid, *J. Phys. Chem. B* 121 (2017) 7173–7179, doi:[10.1021/acs.jpcc.7b05564](https://doi.org/10.1021/acs.jpcc.7b05564).
- [31] R.P. Matthews, T. Welton, P.A. Hunt, Competitive π interactions and hydrogen bonding within imidazolium ionic liquids, *Phys. Chem. Chem. Phys.* 16 (2014) 3238–3253, doi:[10.1039/c3cp54672a](https://doi.org/10.1039/c3cp54672a).
- [32] M. Farren-Dai, S. Cameron, M.B. Johnson, K. Ghandi, Crystal structure and properties of imidazo-pyridine ionic liquids, *J. Comput. Chem.* 39 (2018) 1149–1157, doi:[10.1002/jcc.25091](https://doi.org/10.1002/jcc.25091).
- [33] S.K. Panja, N. Dwivedi, H. Noothalapati, S. Shigeto, A.K. Sikder, A. Saha, S.S. Sunkarie, S. Saha, Significance of weak interactions in imidazolium picrate ionic liquids: spectroscopic and theoretical studies for molecular level understanding, *Phys. Chem. Chem. Phys.* 17 (2015) 18167–18177, doi:[10.1039/C5CP01944C](https://doi.org/10.1039/C5CP01944C).
- [34] B. Baker, C.J. Cockram, S. Dakein, J.M. DeMaria, D.M. George, K.R. Malyk, M.J.F. Sarno, A.J.P. Cardenas, Synthesis and characterization of anilinium ionic liquids: exploring effect of π - π ring stacking, *J. Mol. Struct.* 1225 (2021) 129122, doi:[10.1016/j.molstruc.2020.129122](https://doi.org/10.1016/j.molstruc.2020.129122).
- [35] F. Schroeter, J. Soellner, T. Strassner, Tailored palladate tunable aryl alkyl ionic liquids (TAAILs), *Chem. Eur. J.* 25 (2019) 2527–2537, doi:[10.1002/chem.201804431](https://doi.org/10.1002/chem.201804431).
- [36] M.C. Özdemir, B. Özgün, E. Aktan, 1-Aryl-3,5-dimethylpyrazolium based tunable protic ionic liquids (TPILs), *J. Mol. Struct.* 1180 (2019) 564–572, doi:[10.1016/j.molstruc.2018.12.027](https://doi.org/10.1016/j.molstruc.2018.12.027).
- [37] S. Grimme, J. Antony, S. Ehrlich, H. Krieg, DFT-D3 - A dispersion correction for density functionals, hartree-Fock and semi-empirical quantum chemical methods, *J. Chem. Phys.* 132 (2010) 154104, doi:[10.1063/1.3382344](https://doi.org/10.1063/1.3382344).
- [38] G.M. Sheldrick, A short history of SHELX, *Acta Crystallogr. A* 64 (2008) 112–122, doi:[10.1107/S0108767307043930](https://doi.org/10.1107/S0108767307043930).
- [39] G.M. Sheldrick, Crystal structure refinement with SHELXL, *Acta Crystallogr. C* 71 (2015) 3–8, doi:[10.1107/S2053229614024218](https://doi.org/10.1107/S2053229614024218).
- [40] APEX2, Bruker AXS Inc. Madison Wisconsin USA (2013).
- [41] C.F. Macrae, I.J. Bruno, J.A. Chisholm, P.R. Edgington, P. McCabe, E. Pidcock, L. Rodriguez-Monge, R. Taylor, J. van de Streek, P.A. Wood, Mercury CSD 2.0-new features for the visualization and investigation of crystal structures, *J. Appl. Crystallogr.* 41 (2008) 466–470, doi:[10.1107/S0021889807067908](https://doi.org/10.1107/S0021889807067908).
- [42] L.J. Farrugia, WinGX and ORTEP for Windows: an update, *J. Appl. Crystallogr.* 45 (2012) 849–854, doi:[10.1107/S0021889812029111](https://doi.org/10.1107/S0021889812029111).
- [43] M.J. Frisch, G.W. Trucks, H.B. Schlegel, G.E. Scuseria, M.A. Robb, J.R. Cheeseman, G. Scalmani, V. Barone, B. Mennucci, G.A. Petersson, H. Nakatsuji, M. Caricato, X. Li, H.P. Hratchian, A.F. Izmaylov, J. Bloino, G. Zheng, J.L. Sonnenberg, M. Hada, M. Ehara, K. Toyota, R. Fukuda, J. Hasegawa, M. Ishida, T. Nakajima, Y. Honda, O. Kitao, H. Nakai, T. Vreven, J.A. Montgomery Jr., J.E. Peralta, F. Ogliaro, M. Bearpark, J.J. Heyd, E. Brothers, K.N. Kudin, V.N. Staroverov, T. Keith, R. Kobayashi, J. Normand, K. Raghavachari, A. Rendell, J.C. Burant, S.S. Iyengar, J. Tomasi, M. Cossi, N. Rega, J.M. Millam, M. Klene, J.E. Knox, J.B. Cross, V. Bakken, C. Adamo, J. Jaramillo, R. Gomperts, R.E. Stratmann, O.Yazyev, A.J. Austin, R. Cammi, C. Pomelli, J.W. Ochterski, R.L. Martin, K. Morokuma, V.G. Zakrzewski, G.A. Voth, P. Salvador, J.J. Dannenberg, S. Dapprich, A.D. Daniels, O. Farkas, J.B. Foresman, J.V. Ortiz, J. Cioslowski, D.J. Fox, Gaussian 09, Gaussian, Inc., Wallingford CT, 2010.
- [44] Y. Yamaguchi, M. Frisch, M. J. Gaw, H.F. Schaefer, J.S. Binkley, Analytic evaluation and basis set dependence of intensities of infrared spectra, *J. Chem. Phys.* 84 (1986) 2262, doi:[10.1063/1.450389](https://doi.org/10.1063/1.450389).
- [45] P. Pulay, G. Fogarasi, F.F. Pang, J.E. Boggs, Systematic ab initio gradient calculation of molecular geometries, force constants, and dipole moment derivatives, *J. Am. Chem. Soc.* 101 (1979) 2550–2560, doi:[10.1021/ja00504a009](https://doi.org/10.1021/ja00504a009).
- [46] V.H. Paschoal, L.F.O. Faria, M.C.C. Ribeiro, Vibrational spectroscopy of ionic liquids, *Chem. Rev.* 117 (2017) 7053–7112, doi:[10.1021/acs.chemrev.6b00461](https://doi.org/10.1021/acs.chemrev.6b00461).
- [47] E. Scrocco, J. Tomasi, Electronic molecular structure, reactivity and intermolecular forces: an heuristic interpretation by means of electrostatic molecular potentials, *Adv. Q. Chem.* 11 (1978) 115–193, doi:[10.1016/S0065-3276\(08\)60236-1](https://doi.org/10.1016/S0065-3276(08)60236-1).
- [48] F.J. Luque, J.M. Lopez, M. Orozco, Perspective on electrostatic interactions of a solute with a continuum. a direct utilization of ab initio molecular potentials for the prevision of solvent effects, *Theor. Chem. Acc.* 103 (2000) 343–345, doi:[10.1007/s002149900013](https://doi.org/10.1007/s002149900013).